CONF-960401--41 SAND96-1175C

SELECTIVE OXIDATION OF BURIED AlGaAs FOR FABRICATION OF VERTICAL-CAVITY LASERS

Kent D. Choquette, K. M. Geib, H. C. Chui, H. Q. Hou, and Robert Hull*

Photonics Research Department
Sandia National Laboratories
Albuquerque, NM 87185-0603
kdchoqu@sandia.gov

*University of Virginia
Department of Materials Science
Charlottesville, VI 22903-2442

RECEIVED
JUN 03 1996
OSTI

Abstract

We discuss the selective conversion of buried layers of AlGaAs to a stable oxide and the implementation of this oxide into high performance vertical-cavity surface emitting lasers (VCSELs). The rate of lateral oxidation is shown to be linear with an Arrhenius temperature dependence. The measured activation energies vary with Al composition, providing a high degree of oxidation selectivity between AlGaAs alloys. Thus buried oxide layers can be selectively fabricated within the VCSEL through small compositional variations in the AlGaAs layers. The oxidation of AlGaAs alloys, as opposed to AlAs, is found to provide robust processing of reliable lasers. The insulating and low refractive index oxide provides enhanced electrical and optical confinement for ultralow threshold currents in oxide-apertured VCSELs.

Introduction

Oxide-apertured vertical-cavity surface emitting lasers (VCSELs) have recently demonstrated record low threshold currents[1,2] and threshold voltages[3] at both infrared and visible[4] wavelengths, as well as record high power conversion efficiencies.[5] These advances arise from the reduction of electrical and optical loss due to efficient current injection into the active region[6] and index-guided optical confinement[7] afforded by the buried oxide converted from AlGaAs.[8] The Al-oxide has also been utilized in the fabrication of a variety of other photonic/microelectronic devices, including edge emitting lasers,[9] optical waveguides,[10] and GaAs metal-oxide-semiconductor field effect transistors.[11] Thus understanding the factors which influence the wet oxidation of AlGaAs is important for the development of robust fabrication techniques for advanced optoelectronic devices.

In this paper we discuss the wet oxidation of AlGaAs, the implementation of the oxide in a monolithic VCSEL, and the resulting performance of oxide-apertured VCSELs. We first examine the influence of temperature and composition on the oxidation rate. The oxidation selectivity with respect to Al content is shown to allow the fabrication of buried oxide layers for confinement within the VCSEL. The use of an oxide formed from AlGaAs, rather than from AlAs, is demonstrated to give robust and reliable VCSELs. Finally, the threshold characteristics of oxide-apertured and ion-implanted VCSELs are compared.

DISTRIBUTION OF THIS DOCUMENT IS UNLIMITED MASTER

DISCLAIMER

Portions of this document may be illegible in electronic image products. Images are produced from the best available original document.

Oxidation of AlGaAs

To develop reproducible fabrication processes, wet oxidation of AlGaAs has been examined as a function of Al composition and process parameters. Samples containing AlGaAs layers are subjected to elevated temperatures (350-500°C) in a steam environment. Specifically, a controlled flow of N_2 gas is bubbled through de-ionized water maintained at 82°C and is passed through a three zone tube furnace. Sufficient gas flow is used to insure a water vapor saturated regime so that the resulting oxidation rates are not reactant limited. The lateral oxidation length at 420°C for buried 84 nm thick $Al_xGa_{1-x}As$ layers with x=1.0, 0.98, and 0.92 are plotted in Fig. 1(a). This figure reveals the lateral oxidation obeys a linear rate without an induction time preceding the onset of oxidation. Using a model of silicon oxidation,[12] the oxidation thickness, d_{ox}, achieved in a time t can be calculated from

$$d_{ox}^2 + Ad_{ox} = Bt \quad (1),$$

where B is related to the diffusion constant of reactants through the oxide and B/A is related to the oxidation reaction rate constant. In the limit of short oxidation times and/or thin oxide thickness, equation (1) yields the reaction rate limited case:

$$d_{ox} = (B/A)\, t \quad (2).$$

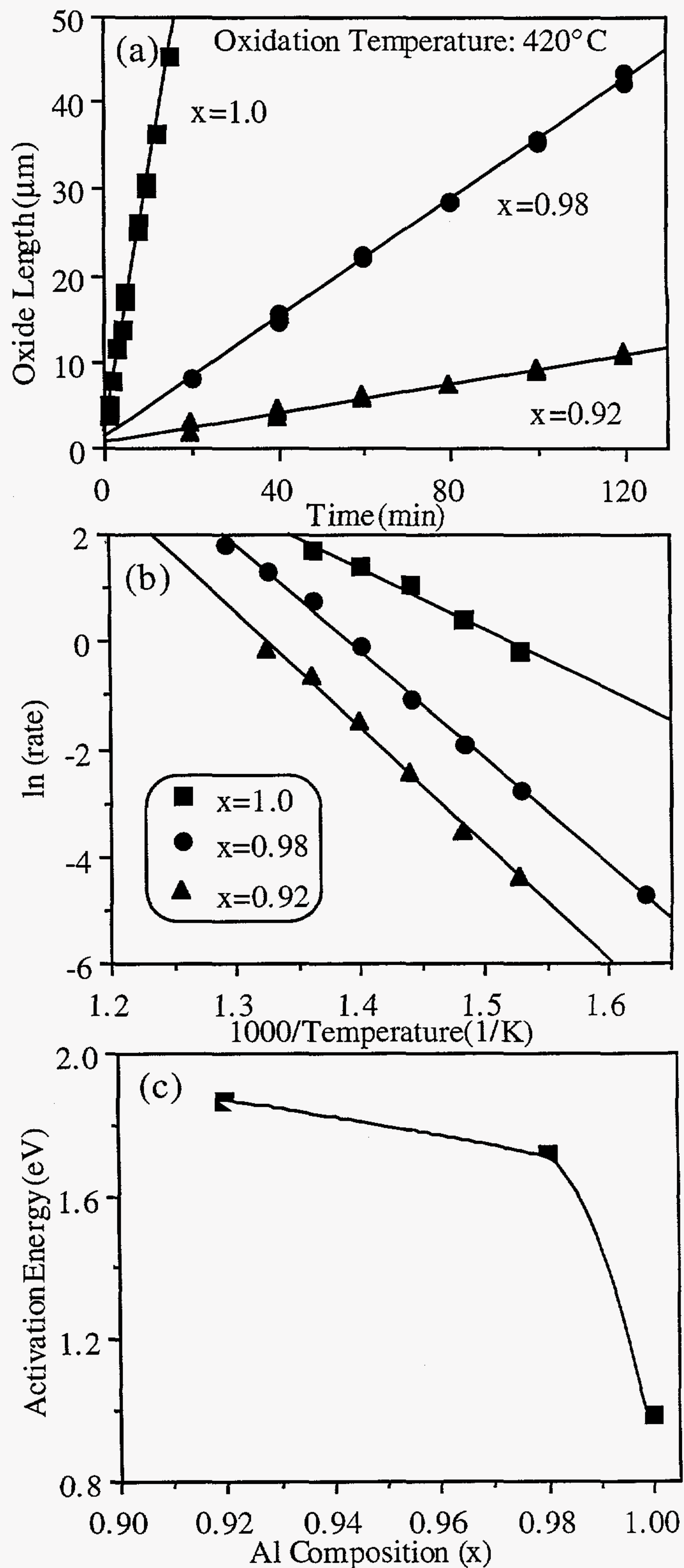

Fig. 1. Wet oxidation of AlGaAs: (a) lateral oxide length; (b) Arrhenius plot of rates; (c) activation energy of oxidation.

For temperatures ranging between 350-500°C linear oxidation rates are observed, which indicate that the lateral oxidation of AlGaAs is rate limited rather than

determined by the diffusion of reactants through the oxide.

The oxidation rate for a specific Al composition depends exponentially on temperature as shown in Fig. 1(b). From this Arrhenius dependence, oxidation activation energies can be calculated and are plotted in Fig. 1(c) for the different AlGaAs alloys. The activation energy for wet oxidation of AlAs is found to be 0.98 eV; in comparison, the wet oxidation activation energy for Si is 1.96 eV.[12] This illustrates the relatively high reactivity of AlAs to oxidation. Notice an increase of the GaAs mole fraction of only 8% nearly doubles the activation energy, producing a value similar to Si. A strong compositional dependence of the oxidation rates follows from the compositional dependence of the activation energies. In fact, the oxidation rate of $Al_xGa_{1-x}As$ for x varying from 1 to 0.8, changes by more than 2 orders of magnitude.[3] Thus a high degree of oxidation selectivity in high Al-containing AlGaAs layers can be obtained with only a minute change in Ga concentration. The oxidation selectivity to Al-content can be exploited for fabrication of buried oxide layers, as described below. However, Fig. 1 also indicates that stringent control of composition and temperature is crucial for attaining a reproducible and selective AlGaAs oxidation processes for device fabrication.

Fabrication of Oxide-Apertured VCSELs

Figure 2 depicts our monolithic VCSEL which employs selective oxidation to produce a buried oxide aperture on each side of the laser active region.[3,13] This oxide-apertured VCSEL structure has several advantages. First, in this monolithic structure we fully exploit low resistance distributed Bragg reflector (DBR) mirror designs (such as parabolic[14] or uniparabolic[15] heterointerface grading in combination with C-doping[16]) in utilizing the entire top mirror to conduct current into the active region. Thus current crowding effects and/or ion implantation damage in the top DBR are avoided. The current apertures immediately surrounding the optical cavity also eliminate sidewall nonradiative recombination present in air-post VCSELs[17] and minimize lateral current spreading outside of the laser cavity. Finally, the smaller refractive index of the oxide layer provides index-guided optical confinement,[7] but in a planar configuration amenable to efficient current flow and heat extraction.

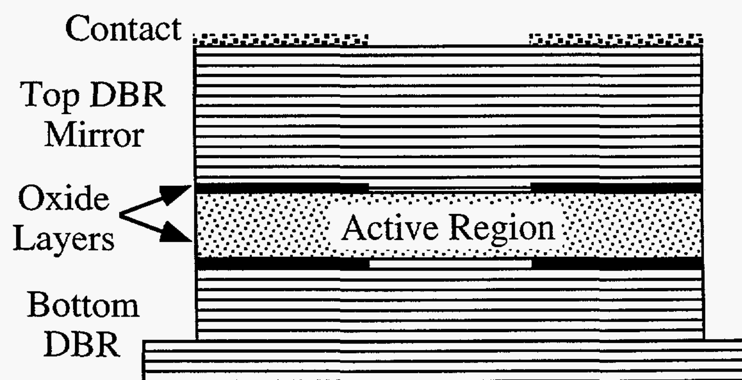

Fig. 2. VCSEL sketch showing the oxidized layers on each side of the active region.

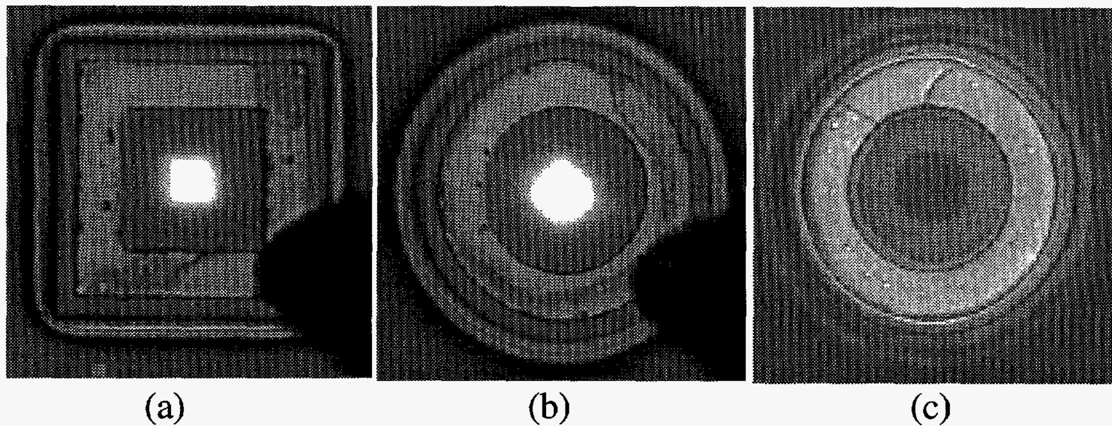

Fig. 3. Top view of VCSELs showing the $Al_xGa_{1-x}As$ current apertures located at the center of the mesas; (a) square mesa emitting light with x=0.98; (b) circular mesa emitting light with x=1.0; (c) circular mesa with x=0.92.

The VCSEL wafers are grown by metalorganic vapor phase epitaxy (MOVPE) in an EMCORE 3200 reactor. This growth technique is especially well suited for selectively oxidized VCSELs due to the complete accessibility of the AlGaAs alloy range, the stringent compositional control, and the high degree of compositional uniformity which can be achieved. The continuous AlGaAs alloy range enables the design of buried oxide layers within the VCSEL by selecting a specific or multiple AlGaAs layer(s) in the VCSEL for oxidation through small variations (≤10%) of the GaAs mole fraction in AlAs. Note that oxidation uniformity requires compositional uniformity. We estimate from our EMCORE oxidation calibration samples that the AlGaAs composition of layers with nominally identical composition vary less than ±0.1%.

Fabrication of oxide-apertured VCSELs[13] begins with the lift-off deposition of a top ring-shaped Ti/Pt/Au p-type contact, and a backside blanket evaporation of a Ge/Au/Ni/Au n-type contact. A silicon nitride mask is deposited on the top surface and patterned to encapsulate the metal contact and form a mesa etch mask. Reactive ion etching employing BCl_3/Cl_2 is used to define the laser mesas, thus forming trenches to expose the mesa sidewalls for oxidation. For the mirror layers not intended for oxidation, we use a GaAs mole fraction of 6 to 8%. The low index layers intended for oxidation adjacent to the optical cavity are adjusted to $Al_{0.98}Ga_{0.02}As$ for an enhanced oxidation rate. The oxidation of VCSELs is typically done at 440°C, producing an oxidation rate of ≈1 µm/min for the $Al_{0.98}Ga_{0.02}As$ layers, which is a factor of 3 or more faster than the surrounding AlGaAs layers. Lastly, the top nitride mask is removed before device testing.

Fig. 3 illustrates top views of oxide-apertured VCSELs. The central regions in the mesa centers correspond to the unoxidized portion of the current aperture which defines the laser cavity. Independent of composition, the current aperture resulting from a square mesa tends to also be square as shown in Fig. 3(a), implying isotropic oxidation. However, for high Al-content layers (x ≥ 0.94) crystallographic dependent oxidation is observed from circular mesas. For example, Fig. 3(b) shows a roughly square aperture results from a circular mesa when oxidizing AlAs. Fig. 3(c) reveals that a circular aperture from a circular

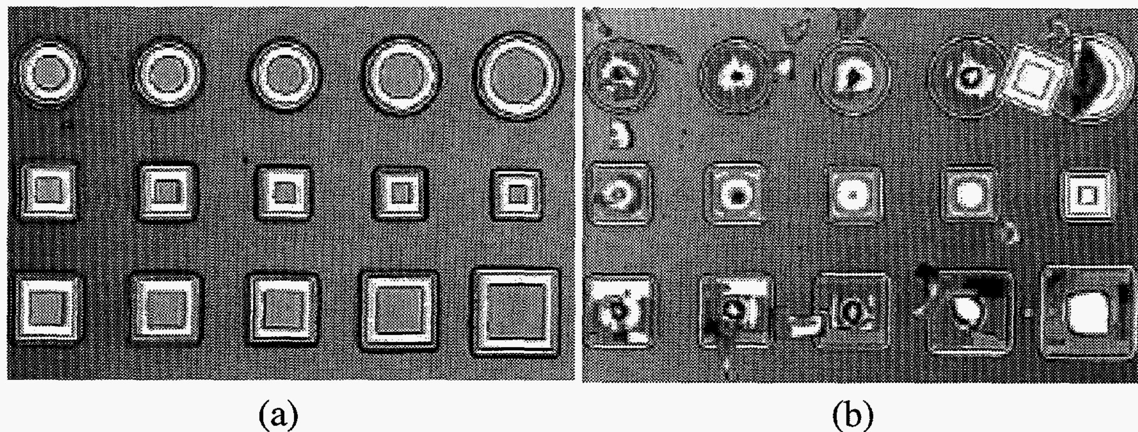

Fig. 4. Top view of VCSEL mesas containing $Al_xGa_{1-x}As$ oxide apertures after rapid thermal annealing to 350°C for 30 sec.; (a) x=0.98; (b) x=1.0.

mesa is regained for an oxide layer composition of x=0.92.

In spite of the crystallographic oxidation, the use of the binary AlAs as the oxidation layer would seem to relax the required compositional control during growth. However, this actually creates new and worse problems. First, the high reactivity of AlAs as seen in Fig. 1 makes control of its oxidation rate problematic. Secondly, structures using oxidized AlAs are mechanically unstable to thermal cycling. Shown in Fig. 4 is a comparison of VCSEL mesas, after rapid thermal annealing to 350°C for 30 seconds, where $Al_{0.98}Ga_{0.02}As$ or AlAs are used in the oxide layers. The mesas containing oxidized AlAs delaminate at the oxide/semiconductor interface, while the mesas with x=0.98 in the oxide layer are unaffected by the anneal. This thermal sensitivity is particularly insidious for post-oxidation VCSEL processing requiring heating to ≈100°C or greater, such as for photolithography, polymer planarization, dielectric deposition, etc. Finally and most importantly, VCSELs using AlAs oxide layers have shown obvious degradation over only a few hours of operation.[18,19]

Cross section TEM images (prepared using focused ion beam etching) of oxide-confined VCSELs using $Al_{0.98}Ga_{0.02}As$ and AlAs as the oxide layers are shown in Figs. 5 and 6, respectively. The terminus of the oxide layer is denoted by the vertical arrows in Figs. 5 and 6, with the unoxidized region beyond this point corresponding to the interior of the laser cavity. In Fig. 5 and all other samples that have been examined which employ $Al_{0.98}Ga_{0.02}As$ oxidation layers, no dislocations or other defects are apparent along the oxide/semiconductor interface or near the oxidation terminus. Moreover, evidence of strain is not apparent, as in Fig. 5. However, near the AlAs oxide terminus in Fig. 6 evidence of a strain field is observed (see contrast at arrow). The strain presumably arises from the volume shrinkage in the oxidized AlAs layer: the γ-Al_2O_3 converted from AlAs experiences a volume contraction of >12% as compared to the original AlAs.[20] By comparison, the oxide shrinkage of $Al_{0.92}Ga_{0.08}As$ has been measured to be only 6.7%.[21] Therefore, the dramatic temperature sensitivity of AlAs samples depicted in Fig. 4, the strain observed at the AlAs oxide terminus in Fig. 6, and the degraded laser lifetimes of VCSELs using AlAs are indicative

Fig. 5. Cross section TEM image (**g**=(311)) of a VCSEL with an $Al_{0.98}Ga_{0.02}As$ oxide layer; the arrow denotes the oxide terminus.

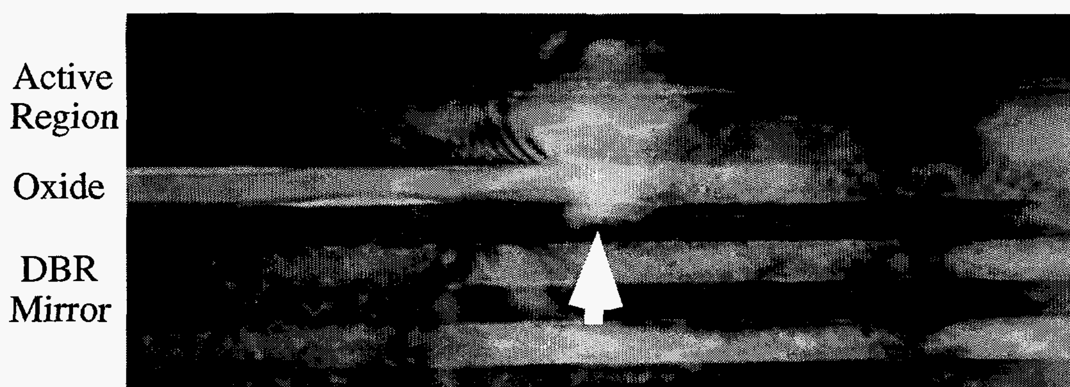

Fig. 6. Cross section TEM image (**g**=(400)) of a VCSEL with an AlAs oxide layer.

of excessive stress in the oxidized structures. To mitigate these adverse effects, the addition of a small amount of Ga to the oxidation layer is found to enable robust oxidation processing and reliable oxide-apertured VCSELs.

Performance of Oxide-Apertured VCSELs

Oxide-apertured VCSELs emitting at 980, 850, 780, and 650 nm have been fabricated and characterized. Shown in Fig. 7 are light-current-voltage curves for 850 and 780 nm devices with 5x5 μm apertures. For many emerging VCSEL applications, such as sources for optical fiber data links, laser printing heads, or free space interconnects, a submilliamp threshold current and an output of ≥ 1 mW is desired. These attributes are depicted in Fig. 7 and have also been demonstrated at 980 nm[3,5,13] and 680 nm[4] using oxide-apertured VCSELs. The improved performance of these VCSELs arises from the enhanced electrical and optical confinement provided by the buried oxide layers.

Figure 8 shows a comparison of oxide-apertured and ion implanted VCSELs fabricated from the same epitaxial wafer. For the latter conventional VCSELs, a deep proton implantation is used to render the material around the laser nonconducting and thus define the laser cavity.[22] For the broad area (>500 μm^2)

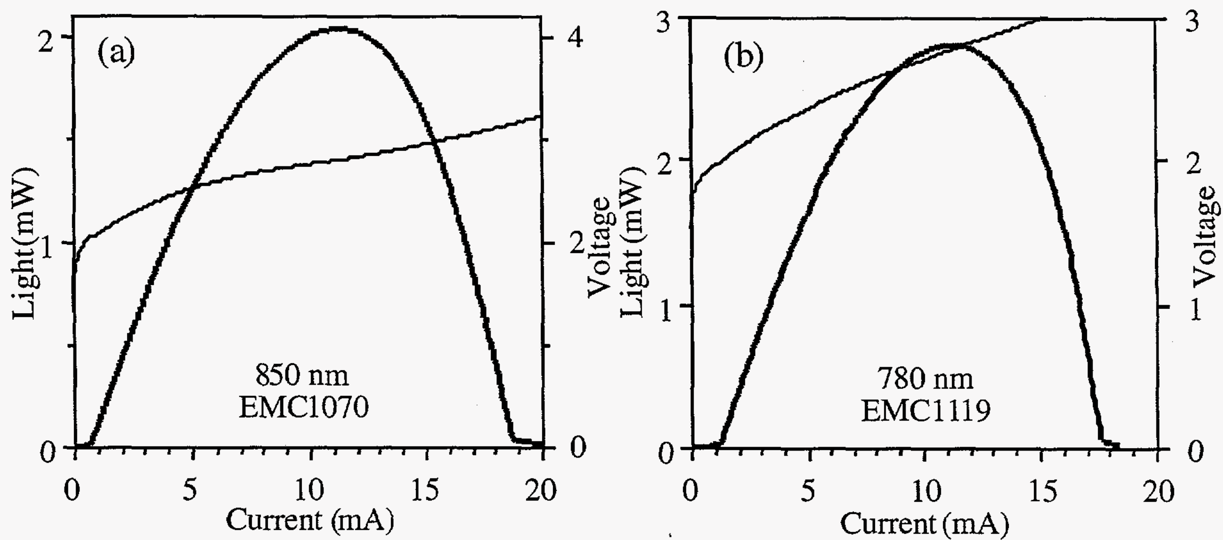

Fig. 7. Characteristics of oxide-apertured VCSELs including output light (heavy curve) and applied voltage (light curve); (a) 850 nm lasing wavelength; (b) 780 nm lasing wavelength.

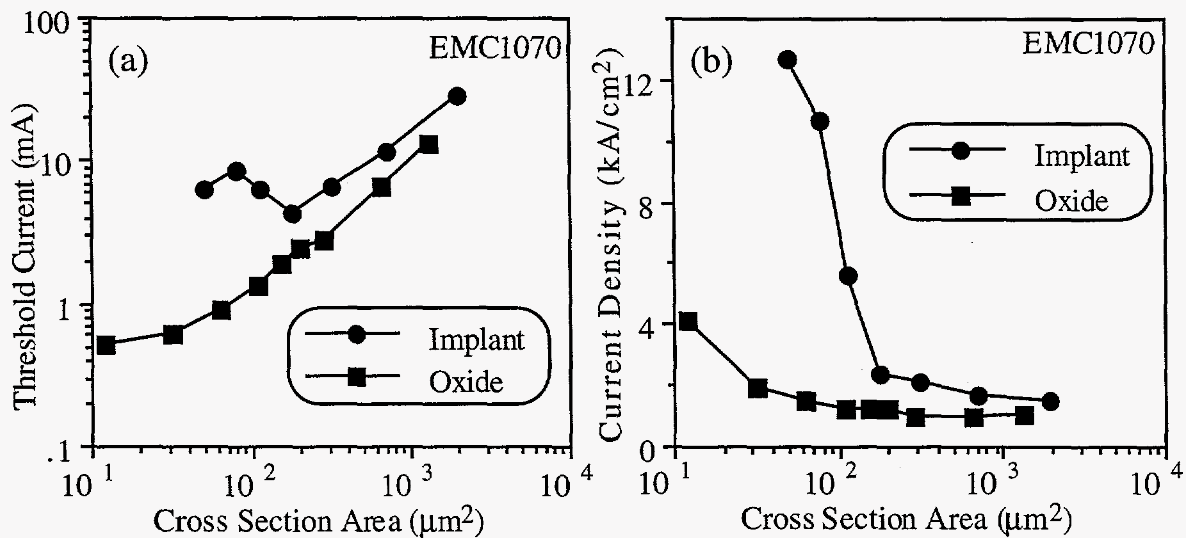

Fig. 8. Threshold properties of 850 nm oxide-apertured VCSELs; (a) threshold current; (b) threshold current density.

lasers in Fig. 8(a), the reduced threshold current of the oxide-confined VCSELs arises due to the improved electrical confinement.[6] Since the insulting oxide layers are located on each side of the active region (see Fig. 2) the charge carriers are efficiently confined and injected into the quantum wells. By comparison, the ion implantation is necessarily located ≈ 0.5 μm above the active region to avoid implantation damage to the quantum wells. Hence significant current spreading outside of the laser cavity occurs, which leads to increased carrier density required for lasing..

Due to the nature of the oxide-apertured VCSELs, extremely small cross section areas approaching 1 μm^2 can be easily fabricated as shown in Fig. 8(a). As a result, threshold currents less than 1 mA are possible for the oxide-apertured VCSELs, as evident in Fig. 8(a) for area ≤ 100 μm^2. Notice the

increase of the threshold current observed for implanted VCSELs in Fig. 8(a) with area ≤ 100 μm^2, which is more pronounced in the threshold current density plotted in Fig. 8(b). The increased threshold current for the implanted VCSELs is needed to form a thermal refractive index profile (thermal "lense") necessary to support a transverse optical mode. The monotonic decrease of the threshold currents apparent for the oxide-apertured VCSELs in Fig. 8(a) is due to the concomitant index-guiding of the buried oxide layer.[7] The refractive index changes from 3.0 for the original AlGaAs layer to ≈1.6 for the oxide, which induces a significant index difference between the laser cavity and the region surrounding the laser thus providing index-guiding optical confinement. For a given laser cross section area, the smaller threshold current density of the oxide-apertured VCSELs in Fig. 8(b) implies that a smaller modal gain is required for the onset of stimulated emission.[23] This is a manifestation of the reduced loss arising from the more efficient confinement of the charge carriers and photons within the laser cavity for the oxide-apertured VCSELs.

Conclusions

Oxidation of AlGaAs alloys may play an important role in advanced optoelectronic device fabrication. We have shown the lateral oxidation rate of buried AlGaAs layers is dependent on temperature and composition. The linear oxidation rates imply a rate limited reaction, and a strong compositional dependence of the oxidation rates is a consequence of the compositional dependence of the activation energies. The oxidation selectivity which is possible with small variations of Ga content in high Al-containing AlGaAs enables the design of devices with buried oxide layers, but also requires stringent control of the alloy compositions for process reproducibility. Finally, the oxidation of AlGaAs alloys is found to provide a structure with less inherent strain than is obtained using AlAs, resulting in robust device processing of reliable VCSELs.

Utilization of buried oxide layers in VCSELs has been shown to have several advantages. The selectively oxidized structure is suitable for fabrication of small active volume microlasers. The insulating oxide efficiently confines and injects charge carriers into the laser quantum wells, while the reduced refractive index of the oxide transversely confines the laser emission. This enhanced electrical and optical confinement enables ultralow threshold currents. Finally, the selectively oxidized structure has been implemented for VCSELs emitting at 980, 850, 780 and 650 nm, indicating the universality of this structure. High performance oxide-confined VCSELs appropriate for a variety of wavelengths should benefit emerging applications and markets being considered for VCSELs.

Acknowledgments

The authors thank R. P. Schneider, Jr., K. L. Lear, and M. Haggerot Crawford for technical discussions and J. Walker of FEI Europe, Inc. for assistance in FIB preparation. This research at Sandia is supported by the U. S. Department of Energy under contract No. DE-AC04-94AL85000.

References

[1]D. L. Huffaker, D. G. Deppe, K. Kumar, and T. J. Rogers, Appl. Phys. Lett. **65**, 97 (1994).

[2]G. M. Yang, M. H. MacDougal, P. D. Dapkus, Electron. Lett. **31**, 886 (1995).

[3]K. D. Choquette, R. P. Schneider, Jr., K. L. Lear, and K. M. Geib, Electron. Lett. **30**, 2043 (1994).

[4]K. D. Choquette, R. P. Schneider, Jr., M. H. Crawford, K. M. Geib, and J. J. Figiel, Electron. Lett. **31**, 1145 (1995).

[5]K. L. Lear, K. D. Choquette, R. P. Schneider, Jr., S. P. Kilcoyne, and K. M. Geib, Electron. Lett. **31**, 208 (1995).

[6]K. D. Choquette, K. L. Lear, R. P. Schneider, Jr., and K. M. Geib, Appl. Phys. Lett. **66**, 3413 (1995).

[7]K. L. Lear, K. D. Choquette, R. P. Schneider, Jr., and S. P. Kilcoyne, Appl. Phys. Lett. **66**, 2616 (1995).

[8]J. M. Dallesasse, N. Holonyak, Jr., A. R. Sugg, T. A. Richard, and N. El-Zein, Appl. Phys. Lett. **57**, 2844 (1990).

[9]J. M. Dallesasse and N. Holonyak, Jr., Appl. Phys. Lett. **58**, 394 (1991).

[10]A. Fiore, V. Berger, E. Rosencher, N. Laurent, S. Theilmann, N. Vodjdani, and J. Nagle, Appl. Phys. Lett. **68**, 1320 (1996).

[11]E. I. Chen, N. Holonyak, Jr., and S. A. Maranowski, Appl. Phys. Lett. **66**, 2688 (1995).

[12]B. E. Deal and A. S. Grove, J. Appl. Phys. **36**, 3770 (1965).

[13]K. D. Choquette, K. L. Lear, R. P. Schneider, Jr., K. M. Geib, J. J. Figiel, and R. Hull, IEEE Photon. Tech. Lett. **7**, 1237 (1995).

[14]R. P. Schneider, Jr., J. A. Lott, M. Hagerott Crawford, and K. D. Choquette, Inter. J. High Speed Electronics and Systems **5**, 625 (1994).

[15]K. L. Lear and R. P. Schneider, Jr., Appl. Phys. Lett. **68**, 605 (1996).

[16]K. L. Lear, R. P. Schneider, Jr., K. D. Choquette, S. P. Kilcoyne, J. J. Figiel, and J. C. Zolper, IEEE Photon. Tech. Lett. **6**, 1053 (1994).

[17]K. D. Choquette, G. Hasnain, Y. H. Wang, J. D. Wynn, R. S. Freund, A. Y. Cho, and R. E. Leibenguth, IEEE Photon. Tech. Lett. **3**, 859 (1991).

[18]D. L Huffaker, J. Shin, and D. G. Deppe, Electron. Lett. **30**, 1946 (1994).

[19]K. D. Choquette, H. Chui, and K. M. Geib, unpublished.

[20]M. H. MacDougal, H. Zhao, P. D. Dapkus, M. Ziari, and W. H. Steier, Electron. Lett. **30**, 1147 (1994).

[21]R. D. Tweston, D. M. Follstaedt, K. D. Choquette, and R. P. Schneider, Jr., submitted to Appl. Phys. Lett. (1996).

[22]Y. H. Lee, B. Tell, K. Brown-Goebeler, J. L. Jewell, and J. V. Hove, Electron. Lett. **26**, 710 (1990).

[23]K. D. Choquette, W. W. Chow, M. Hagerott Crawford, K. M. Geib, and R. P. Schneider, Jr., submitted to Appl. Phys. Lett. (1996).

DISCLAIMER

This report was prepared as an account of work sponsored by an agency of the United States Government. Neither the United States Government nor any agency thereof, nor any of their employees, makes any warranty, express or implied, or assumes any legal liability or responsibility for the accuracy, completeness, or usefulness of any information, apparatus, product, or process disclosed, or represents that its use would not infringe privately owned rights. Reference herein to any specific commercial product, process, or service by trade name, trademark, manufacturer, or otherwise does not necessarily constitute or imply its endorsement, recommendation, or favoring by the United States Government or any agency thereof. The views and opinions of authors expressed herein do not necessarily state or reflect those of the United States Government or any agency thereof.